

## Photoelectron study of SrTiO<sub>3</sub>: An inspection of core-level binding energies with the use of a point-ion model and self-consistent atomic-structure calculations

R. Courths

*Laboratorium für Festkörperphysik, Universität Duisburg, D-4100 Duisburg, West Germany*

J. Noffke

*Institut für Theoretische Physik, Technische Universität Clausthal,  
D-3392 Clausthal-Zellerfeld, West Germany*

H. Wern

*Fachbereich Physik, Universität des Saarlandes, D-6600 Saarbrücken, West Germany*

R. Heise

*Laboratorium für Festkörperphysik, Universität Duisburg, D-4100 Duisburg, West Germany*

(Received 27 March 1990)

The electronic structure of SrTiO<sub>3</sub> has attracted much attention due to its perovskite structure and its surface chemical activity. Perovskite-type compounds are of special interest with regard to the structure-related high- $T_c$  superconductors. We have focused our attention on the effective charges of the cations and the anion, which are reduced relative to their formal ionic charges due to the covalent bonding between O  $2p$  and Ti  $3d$  electrons. Using photoelectron ( $h\nu=100$  eV) core-level shifts observed on TiO<sub>2</sub>- and SrO-plane-terminated (001) surfaces and shifts due to oxygen vacancies ( $V_O$ ), we were able to identify Ti and Sr surface cations and reduced Ti cations in Ti- $V_O$  complexes. Within a simple "localized-hole point-ion" model, the comparison of the experimental binding energies with calculated ionization energies of free ions in different valence states modified by the corresponding Madelung potentials enables us to deduce the effective charges on the Ti ions to be about +2.5 ( $3d^{1.5}$  orbital occupation) in the bulk and about +2.0 ( $3d^2$ ) on the surface, respectively. This conclusion is drawn from the calculated variation of the point-ion energies with the valence-orbital occupation numbers (Ti  $3d^n$ , Sr  $5s^m$ , and O  $2p^{6-m}$ ). The free-ion ionization energies have been obtained from self-consistent-field atomic-structure calculations. Our results for the degree of covalency in the bulk and at the surface are in very good agreement with recent band calculations for the transition metal SrTiO<sub>3</sub>. This further shows that reliable information about the ground state of a solid can be drawn from core-level spectroscopy.

### I. INTRODUCTION

Core-level electron binding energies (BE's) as deduced from photoelectron spectroscopy (PES) are sensitive to local-charge environments and photoelectron (PE) peaks shift as the chemical environment is altered.<sup>1</sup> Often, however, these chemical shifts are small when the formal valence state is changed (e.g., for Cu atoms in the high- $T_c$  superconductors). One of the intentions of core-level PES from solids is the determination of the effective charge state of the atoms in the ground state of the solid. It is questionable whether the integral "formal valence" closely approximates the actual ionic charge it is meant to represent. In materials with largely covalent character the concept of the formal valence loses its relevance, and it is believed that in any real sense valences are not measurable quantities. This question regarding the ionicity or covalency of bonding in solids is of special interest for oxides. Studies referring to this have been performed for iodines,<sup>2</sup> alkaline-earth fluorides,<sup>3</sup> and alkaline-earth oxides.<sup>4-6</sup> Core-level shifts at surfaces and in solids have

been reviewed recently.<sup>7</sup> In this paper we present a study of core-electron BE's in the transition-metal SrTiO<sub>3</sub>, where surface and oxygen-vacancy induced cation BE shifts have been observed.<sup>8,9</sup> In SrTiO<sub>3</sub> the formal valences are clear: the alkaline-earth metal is dipositive, the transition metal is fourfold positive, and oxygen is doubly negative. In this picture the atoms (chemical ions) have closed shells. Our study wants to contribute to the understanding of the term "charge state" (as seen by core ionization) in an oxide with a considerable covalent mixture between the transition-metal (TM)  $3d$  states and oxygen  $2p$  states. It is highly questionable whether the valences are fully ionic or even integral valued.

A crucial question, which we also address here, is the applicability of state-of-the-art electronic band-structure calculations, which treat the many-body Coulomb interactions within the local-density approximation to SrTiO<sub>3</sub>.<sup>10</sup> Band calculations yield nonintegral occupation numbers for valence orbitals within the cation and anion spheres (which are not uniquely defined), and it is interesting whether these "valence-band charges" act on

core electrons as local valence charges in an atomic sense. This seems to be quite natural as seen from the "band-structure perspective." It is therefore astonishing that core-electron binding energies in more or less ionic compounds as oxides are usually ascribed to species in a charge state as deduced from the formal valences.

It is also interesting whether core-level BE's and their shifts yield those ground-state charges predicted from one-electron band calculations, if it is possible to deduce ground-state properties from PES at all. It is well known that core PE peaks, which correspond to the binding energies of occupied core-electron levels, do not directly measure local ground-state charges, for the production of a core hole is always accompanied with relaxations and secondary excitations. In general a PE core spectrum shows a main line with screening of the hole as well as possible, and satellite lines due to excitations of the remaining electron system ("shakeup" and loss satellites). The screening mechanism behind early-transition-metal main lines is under debate<sup>11,12</sup> and will be discussed at the appropriate place. The knowledge of the nature of the final state behind the main line is, of course, of crucial importance to answer the questions posed here.

In this paper we apply, we believe with considerable success, the "localized-hole point-ion" (LHPI) model,<sup>2-5</sup> where screening of the hole left behind occurs via polarization of the surrounding. For bulk SrTiO<sub>3</sub>, for the SrTiO<sub>3</sub>(001) surface (surface core-level shifts), and for oxygen deficient SrTiO<sub>3-x</sub> (defect-induced core-level shifts), we deduce from the Ti 3*p*, Sr 3*d*, and O 1*s* binding energies the effective charges within the cation and anion spheres and the occupation number *n* for Ti 3*d* states. In SrTiO<sub>3</sub> there are band states due to Ti 3*d*-O 2*p* hybridization, which have Ti 3*d* orbital character in the metal sphere. This leads to fractional occupation numbers for the Ti 3*d* states (3*d*<sup>*n*</sup>) and the O 2*p* states (2*p*<sup>6-*m*</sup>). Calculating atomic binding energies (ionization potentials) for core levels in dependence upon the oxidation state of the corresponding free atom (variation of the ground-state occupation number of the valence orbitals) and taking into consideration the corresponding solid-state Madelung potentials, we are able to explain rather consistently the experimental binding energies of the various Ti species observed and to deduce the degree of hybridization (covalency) in the bulk and on the surface in agreement with existent theoretical predictions.<sup>10,13-15</sup>

## II. REVIEW OF EXPERIMENTAL RESULTS ON SrTiO<sub>3</sub>

A survey of the valence electronic structure of SrTiO<sub>3</sub> and its surfaces as deduced from PES up to 1984 is found in the review articles of Henrich<sup>16</sup> and Tsukada, Satoko, and Adachi.<sup>14</sup> Figure 1 schematically shows characteristic results of Ti 3*p*, Sr 3*d*, and O 1*s* core-level, valence-band (VB), and band-gap photoelectron spectra obtained recently from *n*-type SrTiO<sub>3</sub>(001) surfaces taken with synchrotron radiation<sup>8,9</sup> and which are relevant to our considerations. The experimental binding energy is referred to the Fermi level of *n*-type SrTiO<sub>3</sub>, which coincides with the conduction-band minimum.<sup>16</sup>

On stoichiometric and well-ordered surfaces of

SrTiO<sub>3</sub>(001), which can be obtained by annealing a clean surface in oxygen,<sup>8</sup> a surface enhanced covalent mixing of Ti 3*d* and O 2*p* states has been found recently<sup>17</sup> with the use of Ti 3*d* resonant photoemission [quasiatomic Ti 3*p* → 3*d* resonance at  $h\nu=47.5$  eV (Refs. 18 and 19)]. It was found that the surface partial density of Ti 3*d* states extends over the whole valence band and that the low binding-energy portion is of pure surface origin. Another resonant PE investigation of SrTiO<sub>3</sub> (Ref. 20) has not found this surface effect, but could only establish the bulk Ti 3*d* contribution to the high-energy part of the valence band. The occupation of the Ti 3*d* states contributing to the bulk valence band has been experimentally estimated

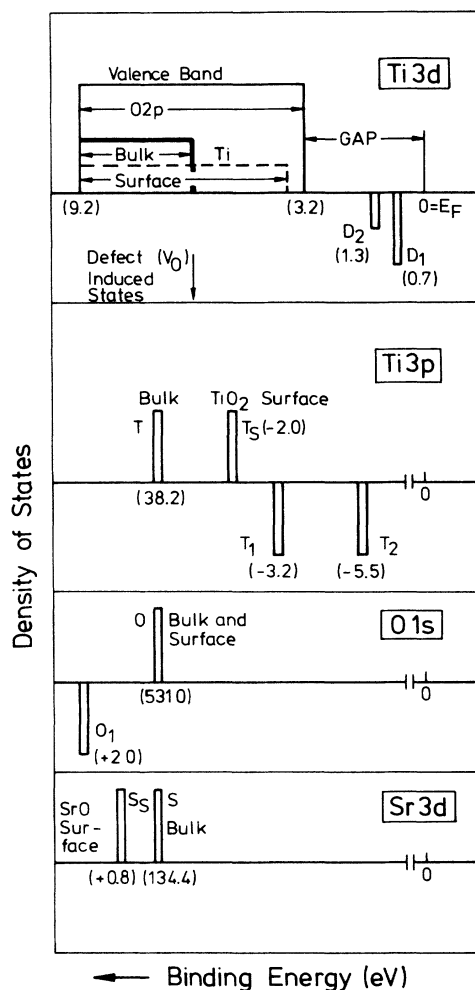


FIG. 1. Schematic representation of the experimental photoelectron spectroscopy results from SrTiO<sub>3</sub>(001) for the Ti 3*d* contribution to the mainly O 2*p*-derived valence band (VB) and to the gap region, and for the Ti 3*p*, Sr 3*d*, and O 1*s* core levels. Upper panels: Bulk and surface binding energies. The index *s* indicates emission from the TiO<sub>2</sub> and SrO terminated surfaces, respectively. Lower panels: Binding energies for species associated with oxygen vacancies (*V*<sub>O</sub>) in the surface region. The numbers below the surface and *V*<sub>O</sub>-induced emissions give the energy shifts relative to the bulk values. Energies are referred to the Fermi level of the *n*-type sample used in experiment.

to  $n=1.4$  (Ref. 17) in rather good agreement with theory.<sup>10</sup> The band-gap region is free from any substantial emission in the case of stoichiometric surfaces,<sup>8-10,17,21,22</sup> on which surface core-level shifts (SCLS) for the Ti 3*p* level<sup>8</sup> and the Sr 3*d* level<sup>9</sup> have been observed, which arise for Ti atom sites in TiO<sub>2</sub>-plane terraces (Fig. 2) and for Sr atom sites in SrO-plane terraces, respectively. The Ti 3*p* (Sr 3*d*) level is shifted to a lower (higher) BE by 2.0 (0.8) eV, whereas the O 1*s* line does not show any splitting due to a surface effect. We will show in this paper that these observations can be understood in terms of the surface-enhanced covalency (SEC), which has been found experimentally<sup>17</sup> and theoretically.<sup>13</sup>

Oxygen-vacancy ( $V_O$ )-rich surfaces, prepared by strong annealing in UHV or ion bombardment, show  $V_O$ -induced Ti 3*p* core emissions  $T_1$  and  $T_2$  at the low binding-energy side of the main-line and band-gap emissions  $D_1$  and  $D_2$  (Fig. 1). The well-known defect gap state  $D_1$  has been associated with Ti<sup>+3</sup> (3*d*<sup>1</sup>) species in the surface region.<sup>21,22</sup> Henrich, Dresselhaus, and Zeiger,<sup>21</sup> and Lo and Somorjai<sup>22</sup> have given an interpretation in terms of charge transfer from oxygen vacancies to neighboring Ti atoms, so that Ti 3*d*-like states are occupied with energies in the gap below the Fermi energy. This interpretation is certainly correct because of the observed resonant enhancement of PE from the gap state,<sup>17</sup> which gives evidence of its Ti 3*d* character. However, an interpretation in terms of integral valence states is doubtful (Henrich, Dresselhaus, and Zeiger and others use the term "Ti<sup>+3</sup>- $V_O$  complexes").

The Ti 3*p* defect emission  $T_1$  ( $\Delta E_B = -3.2$  eV) is very broad and may be the center of more than one overlapping line (possibly three lines as judged from the linewidth of the emission from the unperturbed surface). A low binding-energy shoulder at about  $\Delta E_B = -3$  eV to the Ti 2*p* emission from ion-bombarded or otherwise reduced SrTiO<sub>3</sub> samples has been observed in more bulk-sensitive x-ray photoelectron spectroscopy (XPS) measurements, too, and ascribed to Ti<sup>+3</sup> species adjacent to oxygen vacancies.<sup>23-25</sup> In  $V_O$ -rich surfaces of the comparable compound TiO<sub>2</sub> three defect-induced Ti 2*p* emissions have been found<sup>26</sup> in XPS studies and have been interpreted as representing Ti<sup>+3</sup>, Ti<sup>+2</sup>, and Ti<sup>+1</sup> atoms.<sup>27</sup>

Because of the correlated occurrence of both the core emission  $T_1$  and the gap emission  $D_1$ ,<sup>8</sup> both represent the same reduced Ti species. In a previous paper<sup>8</sup> we have assumed that the line pairs ( $T_1, D_1$ ) and ( $T_2, D_2$ ) in Fig. 1 have their origin in bulk (including the subsurface layer) and surface vacancies, respectively, although this interpretation was not unambiguous. As judged from our calculations presented in this paper, reduced Ti species both in the bulk and in the surface are behind the broad emissions ( $T_1, D_2$ ), and ( $T_2, D_2$ ) probably represent Ti clusters on the surface. An understanding of the surface core-level shift on the "perfect" surface is of crucial importance for the interpretation of the defect-induced shifts in terms of charge states.

Low binding-energy satellites accompany the main lines in the core PE spectra of SrTiO<sub>3</sub>.<sup>11,12,28</sup> Especially the Ti excitations show rather intense satellites at about 14 eV, which play a central part in the several models

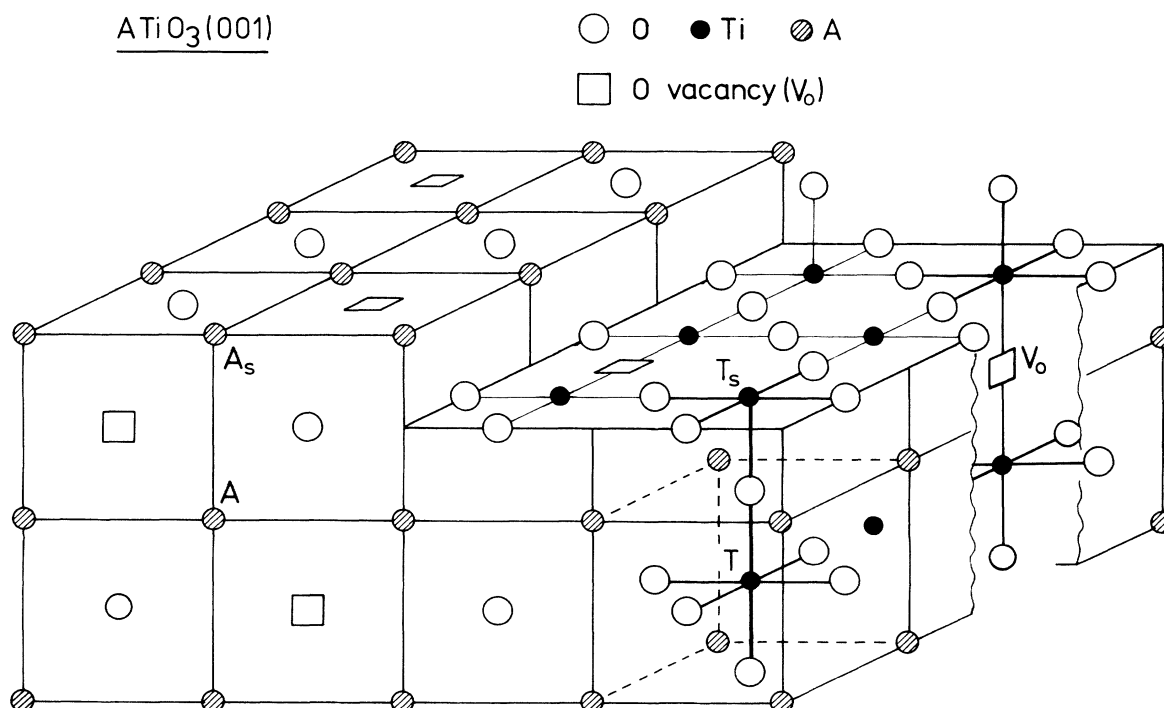


FIG. 2. ATiO<sub>3</sub> cubic perovskite structure and possible ideal surface terminations (TiO<sub>2</sub> and SrO plane, respectively). Oxygen vacancies are also indicated.

developed for the screening in the final state. Because the literature on this field is rather bewildering (references dealing with the early transition metals can be found in the papers of de Boer, Haas, and Sawatzky<sup>11</sup> and Veal and Paulikas<sup>12</sup>), we have performed a reinvestigation of the satellite structure of SrTiO<sub>3</sub>, which will be presented at another place together with inverse photoemission and electron-energy-loss-spectroscopy data.<sup>28</sup> However, for the purpose of the considerations presented in this paper it is important to communicate that both cation and anion satellite structures are so similar, and that an interpretation in terms of energy losses of the photoelectron passing through the sample (plasmon and interband excitations) cannot simply be ruled out as is often done.<sup>11,12</sup> These results encouraged us to use the simple model to be presented in the next chapter.

### III. THE LOCALIZED-HOLE POINT-ION MODEL AND CALCULATIONAL DETAILS

#### A. The model

In order to avoid confusion we call the valence-ionized atoms in their ground state (chemical ions) “atoms” and call the core-ionized atoms “core-ions” or simply “ions.” For the decomposition of core binding energies within the “localized-hole point-ion” (LHPI) model into core-level ionization potentials  $V_{\text{IP}}^0$  of the free atom (chemical ion), Madelung potentials  $E_M$ , and repulsive ( $E_r$ ) and polarization ( $E_p$ ) contributions, we refer the reader to discussions found elsewhere.<sup>2–6</sup> Within this model the binding energy  $E_B$  of a core electron is given by the formula

$$E_B = V_{\text{IP}}^0 - E_M - E_r - E_p. \quad (3.1)$$

The Madelung potential (energy)  $E_M$  is the one-electron energy in the electrostatic field of the surrounding atoms in their ground state, which acts on all levels of one special atom in the same way.  $E_M$  is a positive quantity for cations, but has a negative sign for anions. Thus anions are stabilized and cations are destabilized in the electrostatic field. The ionization potentials  $V_{\text{IP}}^0$  include the intra-atomic relaxation effects of the free atoms upon core ionization and calculational details are given below. Extra-atomic relaxation is included in the polarization term  $E_p$ , whereas the repulsive energy  $E_r$  describes effects due to the compressed atom in the solid as compared to the free atom and also contains some final-state intra-atomic relaxation. The strength of these correction terms will be discussed below. No relaxation effects, such as, e.g., charge transfer from neighboring atoms in the core-ion state, are considered in this model. This may be called into question, but we ask the reader for patience. The results of this simple model presented below may hopefully convince him that no more sophisticated final-state model seems to be necessary to achieve a reliable interpretation of the experimental binding energies of the PE main lines.

#### B. Atomic-structure calculations

The calculations of the ionization potentials are based on a generalized Kohn-Sham theory which applies also to excitations. We performed self-consistent-field (SCF) calculations on various possible states of the respective atoms, where the occupation numbers can be nonintegral to mimic the valence-band charge densities. By taking the differences of the total energies  $E_{\text{tot}}$  for the initial core hole state and the assumed final state we get the  $\Delta$ SCF values for the ionization potentials

$$V_{\text{IP}}^0 = E_{\text{tot}}(C^{-1}v^{n_f}) - E_{\text{tot}}(Cv^{n_i}), \quad (3.2)$$

where  $C$  denotes the core level ( $C^{-1}$  is the core hole),  $v$  is the valence orbital, and  $n_f$  and  $n_i$  are the final and initial occupation numbers, respectively. Since we are only interested in total-energy differences it is sufficient to do atomic-structure calculations for the lighter elements titanium and oxygen within the scalar-relativistic approximation<sup>29,30</sup> instead of solving the Dirac equation as for strontium. Table I shows total energies for free ground-state Ti atoms and it can be seen that the respective values for the total energies differ constantly by about  $6.48 \pm 0.1$  eV and thus cancel in determining the ionization energies. Ionization potentials  $V_{\text{IP}}^0$  for titanium, strontium, and oxygen are given in Tables II–IV. Also given are the free-atom relaxation energies  $E_R^0$ , which are, for a given atom configuration, defined by

$$E_R^0 = E_{\text{tot}}^{\text{frozen}} - E_{\text{tot}}. \quad (3.3)$$

Here  $E_{\text{tot}}^{\text{frozen}}$  is the total energy of the core ion calculated by using the self-consistent (frozen) potential for the respective atom, and  $E_{\text{tot}}$  is the self-consistently calculated total energy of the relaxed core ion.

For the exchange-correlation part  $V_{\text{xc}}^s$  of the potential we have used a nonlocal approximation. The exchange-correlation energy is given by

$$E_{\text{xc}} = \sum_s \int \rho_s(\mathbf{r}) \varepsilon_{\text{xc}}^s(r) d^3\mathbf{r}, \quad (3.4)$$

where the exchange energy per particle,  $\varepsilon_{\text{xc}}(r)$ , depends on the spin-dependent correlation factor  $f_{s's'}(\mathbf{r}, \mathbf{r}')$  by

$$\varepsilon_{\text{xc}}^s(\mathbf{r}) = - \int \frac{\rho_{s'}(\mathbf{r}') f_{s's'}(\mathbf{r}, \mathbf{r}')}{|\mathbf{r}' - \mathbf{r}|} d^3\mathbf{r}'. \quad (3.5)$$

We approximate  $f_{s's'}$  by

$$f_{s's'}(\mathbf{r}, \mathbf{r}') = [1 + \lambda_s(\mathbf{r}) |\mathbf{r}' - \mathbf{r}|^2]^{-5/2}, \quad (3.6)$$

where  $\lambda_s(\mathbf{r})$  is determined by the sum rule

$$\int \rho_{s'}(\mathbf{r}') f_{ss'}(\mathbf{r}, \mathbf{r}') d^3\mathbf{r}' = 1. \quad (3.7)$$

This ansatz for the correlation factor has proven to provide satisfactory results for atomic properties.<sup>31,32</sup> The exchange-correlation potential  $V_{\text{xc}}^s$ , which is defined by

$$\delta E_{\text{xc}} = \sum_s \delta \rho_s(\mathbf{r}) V_{\text{xc}}^s(\mathbf{r}) d^3\mathbf{r}, \quad (3.8)$$

may then be formally written as

$$V_{xc}^s(\mathbf{r}) = 2\varepsilon_{xc}^s(\mathbf{r})$$

$$-\frac{1}{2} \sum_{s', s''} \rho_{s''}(\mathbf{r}) \int \frac{\rho_{s'}(\mathbf{r}')}{|\mathbf{r}' - \mathbf{r}|} \frac{\delta f_{s' s''}(\mathbf{r}', \mathbf{r})}{\delta \rho_s(\mathbf{r})} d^3 \mathbf{r} . \quad (3.9)$$

### C. Madelung potentials for SrTiO<sub>3</sub>

The Madelung potentials for the various lattice sites have been calculated using the method of Tosi.<sup>33</sup> Charge neutrality for the formula unit requires  $q(\text{Ti}) + q(\text{Sr}) + 3q(\text{O}) = 0$ , where the  $q$ 's are the effective charges on the Ti, Sr, and O atoms. In order to achieve charge neutrality for the TiO<sub>2</sub> and SrO planes too, one additionally has to require  $q(\text{Ti}) = 2q(\text{Sr}) = -2q(\text{O})$ . In terms of the valence-orbital occupation numbers  $n(\text{Ti}) \equiv n$  (Ti  $3d^n$ ),  $n(\text{Sr}) \equiv m = n/2$  (Sr  $5s^m$ ), and  $n(\text{O}) \equiv 6 - m$

(O  $2p^{6-m}$ ), one has

$$\begin{aligned} q(\text{Ti}) &= 4 - n = 4(1 - n/4) , \\ q(\text{Sr}) &= 2 - m = 2 - n/2 = 2(1 - n/4) , \\ q(\text{O}) &= -2 + m = -2 + n/2 = -2(1 - n/4) . \end{aligned} \quad (3.10)$$

In this charge distribution model all oxygen sites in the bulk are equivalent as is found in experiment. The bulk Madelung potentials are then given by

$$E_M(n, i) = E_M(0, i)(1 - n/4) , \quad (3.11)$$

where  $E_M(0, i)$  are the Madelung potentials at sites  $i$  (Ti, Sr, O) for all atoms (chemical ions) being in their maximum oxidation state ( $n = 0$ ). The values for  $E_M(0, i)$  at the various sites are given in Table V. The Madelung potentials  $E_M^s$  at lattice sites in the surface of a semiinfinite

TABLE I. Total energies for free ground-state titanium atoms (chemical ions) from self-consistent-field atomic-structure calculations (relativistic and scalar-relativistic, respectively). All values are given in rydbergs.

Atom (chemical ion)	Ground-state valence configuration		$E_{\text{tot}}$ (Ry)	
			Relativistic	Scalar-relativistic
Ti <sup>4+</sup>	$3d^0 4s^0$		-1699.510	-1699.987
Ti <sup>3+</sup>	$3d^1 4s^0$	$d(\frac{3}{2})$	-1702.562	-1703.037
		$d(\frac{5}{2})$	-1702.557	
Ti <sup>2+</sup>	$3d^2$	$d(\frac{3}{2})$	-1704.443	-1704.916
		$d(\frac{5}{2})$	-1704.436	
Ti <sup>1+</sup>	$3d^3$	$d(\frac{3}{2})$	-1705.381	-1705.853
		$d(\frac{5}{2})$	-1705.373	
Ti <sup>0</sup>	$3d^4$	$d(\frac{3}{2})$	-1705.660	-1706.132
		$d(\frac{5}{2})$	-1705.643	
Ti <sup>3+</sup>	$3d^1 4s^1$	$d(\frac{3}{2})$	-1704.263	-1704.738
		$d(\frac{5}{2})$	-1704.259	
Ti <sup>2+</sup>	$3d^2 4s^1$	$d(\frac{3}{2})$	-1701.991	-1702.469
		$d(\frac{5}{2})$		
Ti <sup>1+</sup>	$3d^2 4s^2$	$d(\frac{3}{2})$	-1703.817	-1704.295
		$d(\frac{5}{2})$		
Ti <sup>0</sup>	$3d^3 4s^1$	$d(\frac{3}{2})$	-1703.817	-1704.295
		$d(\frac{5}{2})$		
Ti <sup>1+</sup>	$3d^2 4s^2$	$d(\frac{3}{2})$	-1703.817	-1704.295
		$d(\frac{5}{2})$		
Ti <sup>0</sup>	$3d^3 4s^2$	$d(\frac{3}{2})$	-1703.817	-1704.295
		$d(\frac{5}{2})$		
Ti <sup>1+</sup>	$3d^2 4s^2$	$d(\frac{3}{2})$	-1703.817	-1704.295
		$d(\frac{5}{2})$		
Ti <sup>0</sup>	$3d^2 4s^2$	$d(\frac{3}{2})$	-1703.817	-1704.295
		$d(\frac{5}{2})$		

crystal is calculated using the formula

$$E_M^s = \frac{1}{2}[E_M(n) - E_M^l(n)] + E_M^l(n^s), \quad (3.12)$$

where  $E_M^l$  represents the Madelung potential of a plane parallel to the (001) surface layer. The first term gives the contribution of the bulk (including the subsurface layer). The second term gives the contribution of the surface plane, which is allowed to have reduced charges. The

latter is equivalent with increased valence-orbital occupation numbers at the cations (for Ti,  $n \rightarrow n + \Delta n \equiv n_s$ ; for Sr,  $m \rightarrow m + \Delta m \equiv m_s$ ) and with a decreased occupation number at the anion (for O,  $6 - m \rightarrow 6 - m - \Delta m = 6 - m_s$ ), thus representing a surface-enhanced covalent mixing at the surface.  $\Delta n$  and  $\Delta m$ , respectively, are the surface-bulk differences of the valence-orbital occupation numbers. This effect induces a Madelung shift at the sur-

TABLE II. Ionization potentials,  $V_{\text{IP}}^0 = E_{\text{tot}}(\text{core ion}) - E_{\text{tot}}(\text{atom})$ , and relaxation energies  $E_R^0$  for free titanium atoms (chemical ions). The binding energies,  $E_B = V_{\text{IP}}^0 - E_M$ , for Ti atoms embedded in the electrostatic field of SrTiO<sub>3</sub> (Sr<sup>+2-m</sup>Ti<sup>+4-n</sup>O<sub>3</sub><sup>-2+m</sup> with  $n = 2m$ ,  $E_M$  is the Madelung potential at the corresponding lattice site) are also given. All values are given in eV.

Atom (chemical ion)/ ground-state valence configuration	Ion/core hole	$V_{\text{IP}}^0$	$E_R^0$	$E_B$ (SrTiO <sub>3</sub> )
Ti <sup>4+</sup> /3d <sup>0</sup> 4s <sup>0</sup> ( $n = 0$ )	Ti <sup>5+</sup> /3d	—	—	—
	3p	97.31	1.21	51.70
	3s	121.63	1.36	76.02
	2p	527.89	12.56	482.28
Ti <sup>3+</sup> /3d <sup>1</sup> 4s <sup>0</sup> ( $n = 1$ )	Ti <sup>4+</sup> /3d	41.49	0.79	7.26
	3p	78.22	1.43	43.99
	3s	102.18	1.67	67.95
	2p	504.84	14.02	470.61
Ti <sup>2.5+</sup> /3d <sup>1.5</sup> 4s <sup>0</sup> ( $n = 1.5$ )	Ti <sup>3.5+</sup> /3d	33.19	0.78	4.66
	3p	69.48	1.59	40.95
	3s	93.27	1.88	64.74
	2p	494.56	14.78	466.03
Ti <sup>2+</sup> /3d <sup>2</sup> 4s <sup>0</sup> ( $n = 2$ )	Ti <sup>3+</sup> /3d	25.58	0.76	2.76
	3p	61.36	1.79	38.56
	3s	85.00	2.14	62.18
	2p	485.18	15.55	462.36
Ti <sup>1.9+</sup> /3d <sup>2.1</sup> 4s <sup>0</sup> ( $n = 2.1$ )	Ti <sup>2.9+</sup> /3d	24.14	0.74	2.46
	3p	59.82	1.83	38.14
	3s	83.42	2.20	61.64
	2p	483.42	15.71	461.74
Ti <sup>1+</sup> /3d <sup>3</sup> ( $n = 3$ )	Ti <sup>2+</sup> /3d	12.75	0.62	1.35
	3p	47.42	2.34	36.02
	3s	70.80	2.83	59.40
	2p	469.55	17.08	458.15
Ti <sup>1+</sup> /3d <sup>2</sup> 4s <sup>1</sup>	Ti <sup>2+</sup> /3d	16.36	0.76	4.95
	3p	51.92	1.97	40.51
	3s	75.51	2.35	64.10
	2p	475.39	15.86	463.98
Ti <sup>0</sup> /3d <sup>4</sup> 4s <sup>0</sup> ( $n = 4$ )	Ti <sup>1+</sup> /3d	3.79	0.34	3.79
	3p	37.42	3.07	37.42
	3s	60.66	3.65	60.66
	2p	458.84	18.37	458.84
Ti <sup>0</sup> /3d <sup>2</sup> 4s <sup>2</sup>	Ti <sup>1+</sup> /3d	8.31	0.82	8.31
	3p	43.68	2.23	43.68
	3s	67.25	2.62	67.25
	2p	466.93	16.22	466.93

TABLE III. Ionization potentials  $V_{IP}^0$  and relaxation energies  $E_R^0$  for free Sr atoms (chemical ions) and corresponding binding energies,  $E_B = V_{IP}^0 - E_M$ , for Sr atoms embedded in the Madelung potential ( $E_M$ ) of SrTiO<sub>3</sub>. The ionization energies for 5s screening in the core-hole ground-state,  $V_{IP}^s$  ( $C5s^m \rightarrow C^{-1}5s^{m+1}$ ), are also given. All values are in eV. Relativistic (rel.) and scalar-relativistic (s. rel.) values have been calculated.

Atom (chemical ion)/ ground-state valence configuration	Core hole	$V_{IP}^0$		$E_R^0$	$E_B = V_{IP}^0 - E_M$	$V_{IP}^s$
		s. rel.	rel.			
Sr <sup>2+</sup> /5s <sup>0</sup> ( $m=0$ )	4p	41.08		0.90	21.21	21.84
	4p( $\frac{1}{2}$ )		41.99		22.12	
	4p( $\frac{3}{2}$ )		40.68		20.81	
	4s	59.88		1.42	40.01	40.54
	4s		59.74		39.87	
	3d	153.37		8.78	133.71	133.71
	3d( $\frac{3}{2}$ )		154.56		134.69	
Sr <sup>1+</sup> /5s <sup>1</sup> ( $m=1$ )	4p	33.18		1.43	23.25	20.58
	4s	51.89		1.99	41.96	39.22
	3d	145.07		9.48	135.14	132.14
Sr <sup>0</sup> /5s <sup>2</sup> ( $m=2$ )	4p	26.31		2.14	26.31	
	4s	44.95		2.85	44.95	
	3d	137.91		10.37	137.91	

TABLE IV.  $V_{IP}^0$ 's, relaxation energies  $E_R^0$ , and binding energies  $E_B = V_{IP}^0 - E_M$ (SrTiO<sub>3</sub>) for free-oxygen atoms. The values of Broughton and Bagus (Refs. 6 and 7) are given for comparison (in parentheses). All values are given in eV.

Atom (chemical ion)/ ground-state valence configuration	Ion/valence or core hole	$V_{IP}^0$	$E_R^0$	$E_B$
O <sup>0</sup> /2p <sup>2</sup> 12p <sup>2</sup> 1 ( $m=2$ )	O <sup>1+</sup> /2p <sup>1</sup> 5 <sup>1</sup> 2p <sup>1</sup> 5 <sup>1</sup>	15.63	2.86	15.63
	2s <sup>1</sup>	29.55	3.78	29.55
$E_{tot} = -149.6763$ Ry	1s <sup>1</sup>	545.13	21.42	545.13
	1s <sup>1</sup>	(545.04)		(545.04)
O <sup>1-</sup> /2p <sup>2</sup> 5 <sup>1</sup> 2p <sup>2</sup> 5 <sup>1</sup> ( $m=1$ )	O <sup>0</sup> /2p <sup>2</sup> 12p <sup>2</sup> 1	3.01	3.67	14.92
	2s <sup>1</sup>	16.75	5.63	28.66
$E_{tot} = -149.8813$ Ry	1s <sup>1</sup>	529.05	25.88	540.96
	1s <sup>1</sup>	(528.15)		(540.05)
O <sup>1 2-</sup> /2p <sup>2</sup> 6 <sup>1</sup> 2p <sup>2</sup> 6 <sup>1</sup> ( $m=0.8$ )	O <sup>0 2-</sup> /2p <sup>2</sup> 112p <sup>2</sup> 11	0.94	4.02	15.23
	2s <sup>1</sup>	14.60	6.41	28.89
$E_{tot} = -149.8498$ Ry	2s <sup>1</sup>	526.53	41.64	540.82
O <sup>2-</sup> (Ref. 6) ( $m=0$ )	O <sup>1-</sup> /2p <sup>5</sup>	(-8.50)		(15.31)
	1s <sup>1</sup>	(517.75)		(541.56)

TABLE V. Madelung potential parameters in the bulk and in the TiO<sub>2</sub>- and SrO-plane terminated surfaces of SrTiO<sub>3</sub>(001) as defined in Eqs. (3.11) and (3.13). All values are given in eV.

Site	Bulk	Plane	Surface	
	$E_M(0)$	$E_M^p(0)$	$\Delta E_M(0)$	$C_M$
Ti	+45.64	+40.68	-2.48	-10.17
O(TiO <sub>2</sub> plane)	-23.81	-23.83	0	+5.96
Sr	+19.87	+16.85	-1.51	-4.21
O(SrO plane)	-23.81	-16.85	+3.48	+4.21

face given by

$$\Delta E_M = E_M^s - E_M = \Delta E_M(0)(1 - n/4) + C_M \Delta n. \quad (3.13)$$

The values  $\Delta E_M(0)$  and  $C_M$  for the various sites are given in Table V.

Our Madelung potentials are in nearly perfect agreement with those calculated by Wolfram, Kraut, and Movin<sup>34</sup> for SrTiO<sub>3</sub>. According to their result the electrostatic potential approaches its bulk value one layer in from the surface, as has been found in a similar calculation performed for TiO<sub>2</sub>.<sup>35</sup> Thus, atoms in the second layer are already indistinguishable from bulk atoms. With the exception of the oxygen site in a TiO<sub>2</sub> surface plane of SrTiO<sub>3</sub>, in all cases the Madelung potential at an atomic site in the surface layer is smaller in magnitude than in the bulk. Thus in the surface, electrons at cation sites are more deeply bound and those at anion sites are less bound than in the bulk. This effect is still increased if the charge on surface atoms is decreased. Watson *et al.*<sup>35</sup> have already pointed out, that the elucidation of information about the chemical state of surface atoms requires the consideration of Madelung effects.

We have neglected surface reconstructions found in a recent low-energy electron diffraction (LEED) analysis of SrTiO<sub>3</sub>.<sup>36</sup> According to this study the oxygen ions are pulled out of both possible surfaces (see Fig. 1) by  $s(\text{TiO}_2) = 0.08 \text{ \AA}$  and  $s(\text{SrO}) = 0.16 \text{ \AA}$ , combined with a relaxation of the first two layer distances,  $d_{12}(\text{TiO}_2)/d_0 = (+2 \pm 2)\%$  and  $d_{12}(\text{SrO})/d_0 = (-10 \pm 2)\%$ , respectively. The vertical oxygen displacements produce a reduction of the Madelung energies for surface ions by about 1% per nearest neighbor and can be neglected. The layer relaxations cause shifts of about +0.2 eV for the ions in the TiO<sub>2</sub> surface which does not affect the conclusions drawn below. For the oxygen ions in the SrO surface there is no shift because both effects cancel each other. The Sr surface ions are shifted by at most 0.5 eV to lower BE's which also will be neglected because other correction terms discussed below are more severe.

#### D. Correction terms in the electrostatic model

The polarization correction (extra-atomic screening) to the binding energies in the simple electrostatic model [Eq. (3.1)] is an important one to include.<sup>2</sup> Polarization is a final-state effect, since before ionization takes place each ion is in a symmetric environment. After core-electron ejection, the electrons on neighbor atoms relax in the direction of the core ion, thereby lowering the total energy. The binding energies are shifted to lower values. For TiO<sub>2</sub> de Boer, Haas, and Sawatzky<sup>11</sup> have estimated a polarization energy  $E_p = 4 \text{ eV}$  for Ti 2*p* core holes, a value which we use here as a guide.

The repulsion correction  $E_r$  includes both initial- and final-state effects.<sup>2-7</sup> When the chemical ion is placed into a point-charge field, the valence orbitals are compressed and the core levels are shifted up in energy. The final-state contribution is an increase of the binding energy because due to the smaller size of the core ion the valence orbitals has a place to expand. Mahan<sup>4,5</sup> has

shown that these repulsive energies for alkaline-earth cations in chalcogenide crystals can be neglected, whereas for anions repulsive corrections of about some eV have to be taken into account. The latter results has also been found by Broughton and Bagus.<sup>6</sup>

#### E. Binding energies in a local screening model

Transition-metal (TM) final-state screening by a 3*d* electron that locally resides at the cation site has been proposed for the main lines of early TM's in insulators by Veal and Paulikas.<sup>12</sup> In their relaxation model with local screening (a behavior which is well known from metals), the presence of a core hole pulls down unfilled eigenlevels which then become populated due to charge transfer from neighboring ligands to locally charge compensate the core hole. This process decreases the binding energy of the PE main line. Thus, Veal and Paulikas<sup>12</sup> interpret the TM main line as arising from a 3*d*-screened final state,  $C 3d^n \rightarrow C^{-1} 3d^{n+1} L^{-1} + e_{\text{photo}}^-$ , where the screening electron is supplied by the ligands *L*. The effect of such a process on the ligands energetics has not been considered by these authors. In order to test this model we have calculated these "screened" ionization energies ( $V_{\text{IP}}^s$ ) given by

$$E_B = V_{\text{IP}}^s = E_{\text{tot}}(C^{-1}, v_1^n v_2^1) - E_{\text{tot}}(C, v_1^n v_2^0), \quad (3.14)$$

where  $v_1$  represents the atomic valence orbitals occupied with *n* electrons in the ground state (Ti 3*d*<sup>*n*</sup>, Ti 3*d*<sup>2</sup>4*s*<sup>1</sup>, . . .), and  $v_2$  represents the screening orbital (3*d*, 4*s*, 4*p*, 4*d*) occupied with one electron after core ionization. The final-state occupation of the outer 4*s*, 4*p*, and 4*d* orbitals simulates less locally screened core-hole states.<sup>37</sup>

#### IV. COMPARISON OF EXPERIMENTAL AND THEORETICAL BULK BINDING ENERGIES

In Figs. 3–7 calculated binding energies are compared with the experimental ones which are referred to the Fermi energy being the position of the least bound electron. A discussion of the reference-level problem in metallic and insulating systems is found in Refs. 2, 3, 6, 7, and 38 and there seems to be no unanimous opinion about the appropriate reference level. Recently Eckardt and Fritsche<sup>38</sup> have shown that the Fermi level is the built-in reference level in calculations of our type for local excitations in metals. *n*-type SrTiO<sub>3</sub> behaves as a metal because a low density of oxygen vacancies is always present and no charging effects have been observed.

Figure 3 shows free atom Ti 3*p*-level binding energies for "atomic" Ti<sup>2+</sup> (3*d*<sup>2</sup>) in comparison with the experimental value in SrTiO<sub>3</sub>. This oxidation state has been chosen because the free-atom BE just agrees with the experimental one for SrTiO<sub>3</sub> after correction for the corresponding Madelung potential [Eq. (3.1)] for Sr<sup>1+</sup>Ti<sup>2+</sup>O<sub>3</sub><sup>1-</sup>. The figure also shows that a locally 3*d*-screened final state [ $V_{\text{IP}}^s(3d^3)$ ] gives a too low BE, whereas a less local screening via Ti 4*s*, *p*, or *d* states may explain the experimental BE, too. One already recognizes that within the electrostatic model the comparison



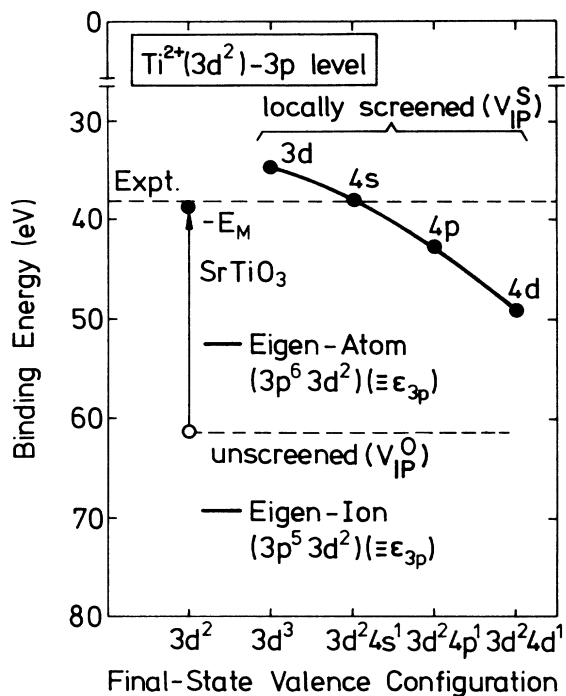


FIG. 3. Calculated ionization potentials at the Ti  $3p$  level for the chemical ion (“atom”)  $\text{Ti}^{2+}(3d^2)$ . The energy marked “unscreened” results for core ionization of the isolated atom,  $V_{\text{IP}}^0 = E_{\text{tot}}(3p^5 3d^2) - E_{\text{tot}}(3p^6 3d^2)$ . This energy falls approximately midway between the calculated single-electron  $3p$  eigenvalue  $\epsilon_{3p}$  for the ground state (“eigen-atom”) and the core-hole state (“eigen-ion”), respectively. The energies marked “locally screened” represent ionization energies for a screened hole state (simulating the “core ion” in a bulk supplying screening charges) with the singly occupied screening orbitals  $v$  indicated,  $V_{\text{IP}}^S = E_{\text{tot}}(3p^5 3d^2 v^1) - E_{\text{tot}}(3p^6 3d^2)$ . The effect of the Madelung potential  $E_M$  in  $\text{SrTiO}_3$  on the electron removal energy is indicated by the arrow. The dashed line gives the experimental Ti  $3p$  bulk binding energy.

between theory and experiment leads to a rather high covalency in  $\text{SrTiO}_3$  with much lower oxidation states than the formal ones ( $\text{Ti}^{4+}$ , etc.), irrespective of which kind of screening is behind the main line. Figure 3 also shows eigenvalues at the Ti  $3p$  core level for the ground state of the  $\text{Ti}^{2+}$  atom (called eigen-atom in Fig. 3) and for the bare core-ionized atom (eigen-ion). The binding energy  $V_{\text{IP}}^0$  is approximately midway between the two eigenvalues, demonstrating that local-density eigenvalues are very different from ionization energies.<sup>39</sup>

Figure 4 shows bare ( $V_{\text{IP}}^0$ ) and screened ( $V_{\text{IP}}^S$ ) Ti  $3p$  binding energies for atomic titanium with the valence-electron configurations  $3d^n$  and  $3d^n 4s^{n-2}$  ( $n=3,4$  in the latter case), respectively. The occupation number  $n$  simulates the degree of chemical ionization in the ground state ( $+4-n$  is the charge state). As expected, the  $V_{\text{IP}}^0$ 's for reasonable charge states between  $+4$  and  $+2$  are far away from experiment. A locally  $3d$ -screened final state gives too low binding energies for all ground-state configurations  $3d^n$ . Furthermore, the  $V_{\text{IP}}^S$ 's have to be decreased by some eV due to the compressional effects,

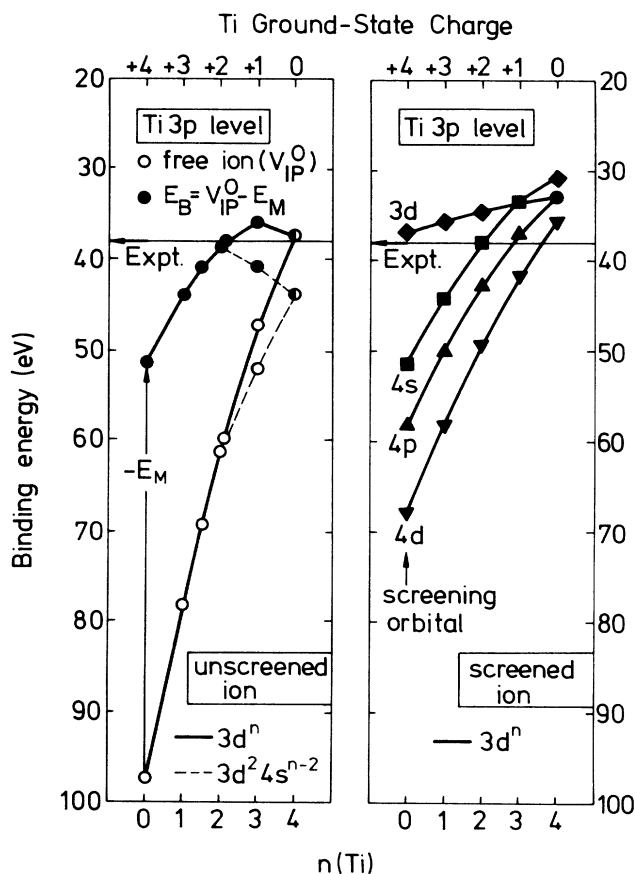


FIG. 4. Left: Dependence of the unscreened ionization energies  $V_{\text{IP}}^0$  (electron removal energies, unfilled circles) of the Ti  $3p$  level on the ground-state valence-electron occupation number  $n$  [ $3d^n$  and  $3d^n 4s^{n-2}$  ( $n=3,4$ ), respectively] of the free titanium atom (chemical ion). The binding energies  $E_B = V_{\text{IP}}^0 - E_M$  for a single electron in the “bare” atom in the electrostatic field of  $\text{SrTiO}_3$  ( $E_M$  is the Madelung potential) are also shown as solid circles. Right: Dependence of the screened Ti  $3p$  ionization potentials  $V_{\text{IP}}^S$  on  $n$ . The values labeled  $3d$ ,  $4s$ ,  $4p$ , and  $4d$  are total-energy differences between the ground state ( $3p^6 3d^n$  or  $3p^6 3d^n 4s^{n-2}$ ) and the final state containing a  $3p$  core hole ( $3p^5$ ) and an additional occupied  $3d$ ,  $4s$ ,  $4p$ , or  $4d$  screening electron orbital ( $3p^5 3d^2 3d^1$ , etc.)

which act irrespective of which model is used for the final state. So we have the first hint that the  $3d$ -screening model does not properly describe the experiment. However, less locally screened states (via  $4s$  or  $4p$  occupation) may describe the experimental values rather well for ground-state configurations between  $3d^1$  and  $3d^2$ . Such values for the ground-state  $3d$ -orbital occupation are also predicted in the electrostatic model, which is in perfect agreement with experiment for the  $\text{Ti}^{2+}(3d^2)$  ground-state atom if one neglects polarization and compression corrections. Due to the latter contributions to the binding energy, our results for the Ti  $3p$ ,  $3s$ , and  $2p$  levels (Figs. 4 and 5) strongly point to an effective ground state of about  $\text{Ti } 3d^{1.5}$ , with  $3d^2$  and  $3d^1$  as upper and lower limits, respectively.

If the reader prefers referring a binding energy to the

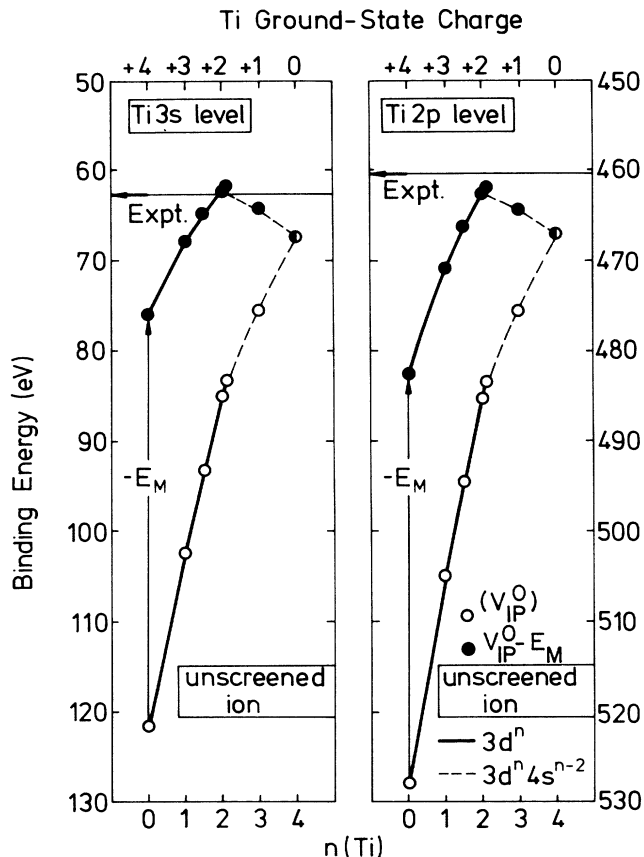


FIG. 5. Ionization energies  $V_{IP}^0$  for the Ti 3s and Ti 3p levels and corresponding binding energies  $E_B = V_{IP}^0 - E_M$  in  $\text{SrTiO}_3$ . Compare with Fig. 4.

vacuum level of a sample, defined as the energy for an electron at the Fermi level to escape from the solid, the work function of about 4 eV (Refs. 21, 22, and 28) has to be added to the experimental values shown in Figs. 4–7. This would give somewhat higher effective charges by about +0.5 for the titanium atoms. However, the main conclusions about the effective valences are drawn from binding-energy differences and shifts presented below, where the reference-level problem is minimized.

In case of outer orbital screening, presumably some kind of Madlung-potential correction must be performed too, because 4s, 4p, and 4d screening only perform partial charge compensation of the core hole. Such kind of correction would shift the calculated binding energies  $V_{IP}^s$  to lower values, such that the Ti 3d ground-state occupation as derived from the experiment-theory comparison would be lower than that derived from uncorrected  $V_{IP}^s$ 's.

According to de Boer, Haas, and Sawatzky<sup>11</sup> the titanium main lines correspond to nonlocal screened core holes, where screening is achieved by ligand polarization towards the anion, if hybridization between metal *d* states and anion *p* states is neglected. In this simple case, their screening mechanism is identical with that in the LHPI model. However, de Boer, Haas, and Sawatzky show that inclusion of covalent bonding complicates the situa-

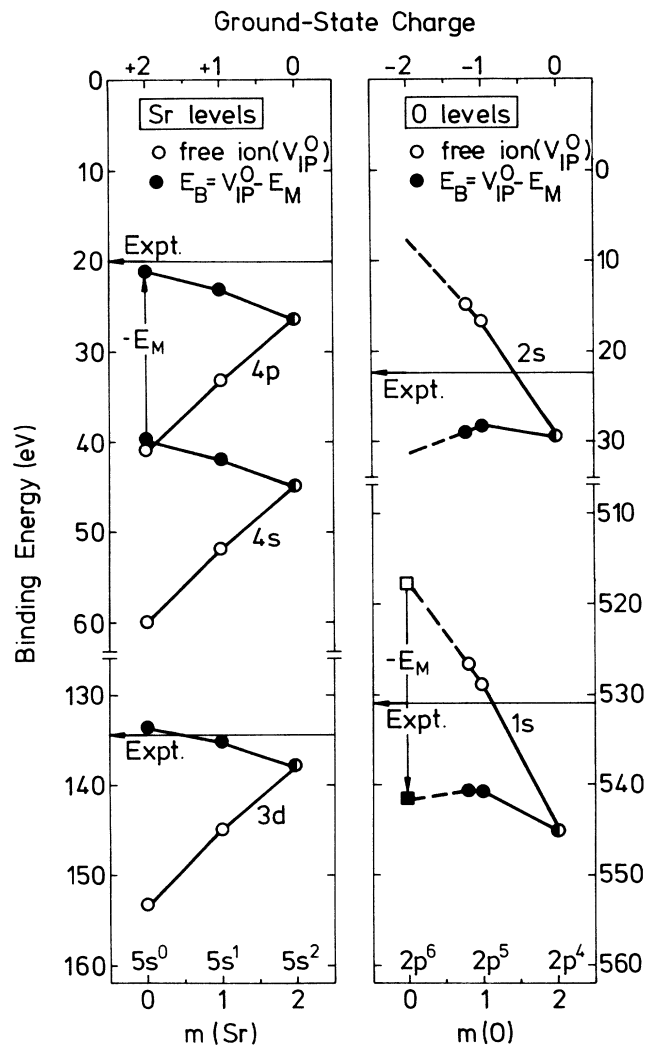


FIG. 6. Left: Dependence of the unscreened ionization energies  $V_{IP}^0$  for the Sr 4p, 4s, and 3d levels on the ground-state valence-electron occupation number of the free Sr atom (chemical ion,  $\text{Sr } 5s^m$ ) and the corresponding binding energies  $E_B = V_{IP}^0 - E_M$  ( $E_M$  is the Madlung potentials in  $\text{SrTiO}_3$ ). Right: Same for the oxygen 1s and 2s levels. The  $\text{O}^{2-}$  energy  $V_{IP}^0$  (open square) is taken from Broughton and Bagus (Refs. 6 and 7). The experimental values for  $\text{SrTiO}_3$  are indicated by arrows.

tion. In their extended model, the Ti core hole is partially screened with 3d electrons in its final ground state, in contrast to the LHPI model.

The validity of the simple electrostatic model is further supported by results of recent band-structure calculations,<sup>10</sup> from which a Ti 3d contribution to the valence band of about 1.7 electrons has been derived. This Ti 3d valence configuration is in excellent agreement with the estimate drawn from Fig. 4 within the framework of the simple LHPI model.

The situation is not so favorable for oxygen and strontium (Fig. 6). In the case of  $\text{Sr}(5s^m)$ , the binding energies in the point-ion model are again near to the experiment. However, because of the weak dependence on the occupa-

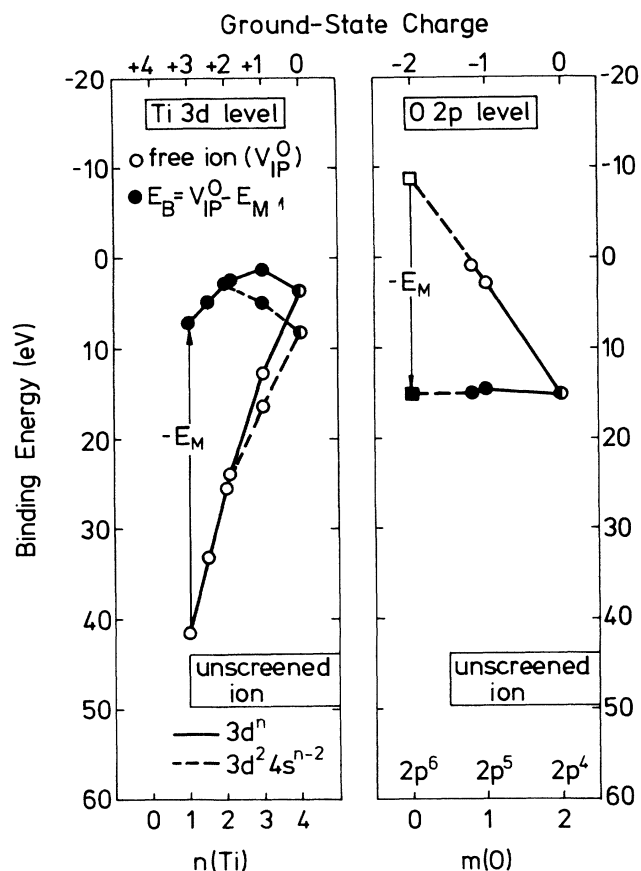


FIG. 7. Same as in Figs. 4, 5, and 6 for the Ti 3d and O 2p levels, respectively.

tion number  $m$ , and taking into account the BE decreasing correction terms, no precise statement about the effective oxidation state can be given. It has to be noticed, too, that the BE's in the screening model ( $V_{IP}^S$  in Table III) are also close to experiment. Because the point-ion BE's for  $Sr^{2+}(5s^0)$  are too near to the experimental values, one might conclude from Fig. 6 that at least one valence electron occupies the Sr 5s orbital. This estimate is supported by a comparison of the Sr 3d BE's (average) in SrTiO<sub>3</sub> (the binding energy is 134.4 eV, Fig. 1) with those in SrO [the binding energy is 135.7 eV (Ref. 40)] and Sr metal [the binding energy is 134.9 eV (Ref. 40)], which shows that the former are much closer to the metal than to the oxide (within an experimental error of about 0.5 eV).

The oxygen O 1s binding energy in oxides represents a well-known mystery.<sup>6</sup> most O 1s BE's exist near 530 eV and are apparently independent of the Madelung potential.<sup>6</sup> Even oxides with two different oxygen sites exhibit only one O 1s peak. But this is only in contradiction to Madelung arguments if one assumes the same valence states (e.g., the formal one -2) and if compressional corrections are neglected. Broughton and Bagus<sup>6</sup> have shown that compressional shifts act in the opposite direction to Madelung shifts, and that a large Madelung potential does indeed produce a large compression of the anion's valence shell. Figure 6 shows that the "point-

ion" O 1s BE is about 10 eV higher than the experimental value and is apparently independent of the 2p occupation. This result must be taken with some caution because the  $O^{-2}$  value, which is taken from Ref. 6, is in doubt since the free atom  $O^{-2}$  is not stable in theory or in experiment. The situation is likewise uncertain for the O 2s level. Thus we cannot determine the effective oxygen charge from absolute binding energies.

For completeness, Fig. 7 shows corresponding results for the Ti 3d and O 2p levels, although it is questionable to compare binding energies of delocalized valence levels with theoretical energies for the free atoms. The SrTiO<sub>3</sub> valence band (VB) extends from 3.2 to 9.0 eV (Fig. 1), and the theoretical point-ion O 2p BE's are too low in energy, as are those for O 2s and O 1s. For all three oxygen levels an increase of the calculated energies by about 9 eV would fit the experiment independent from the valence configuration. The experimental Ti 3d contribution to the bulk VB is found in the high BE part at about 6–9 eV.<sup>17</sup> The point-ion BE's, if applicable to VB states for Ti 3d ground-state occupation with about 1.5 electrons, are a bit too low as compared to experiment.

Citrin and Thomas<sup>3</sup> have already pointed out that a reasonable way to minimize deviations between theory

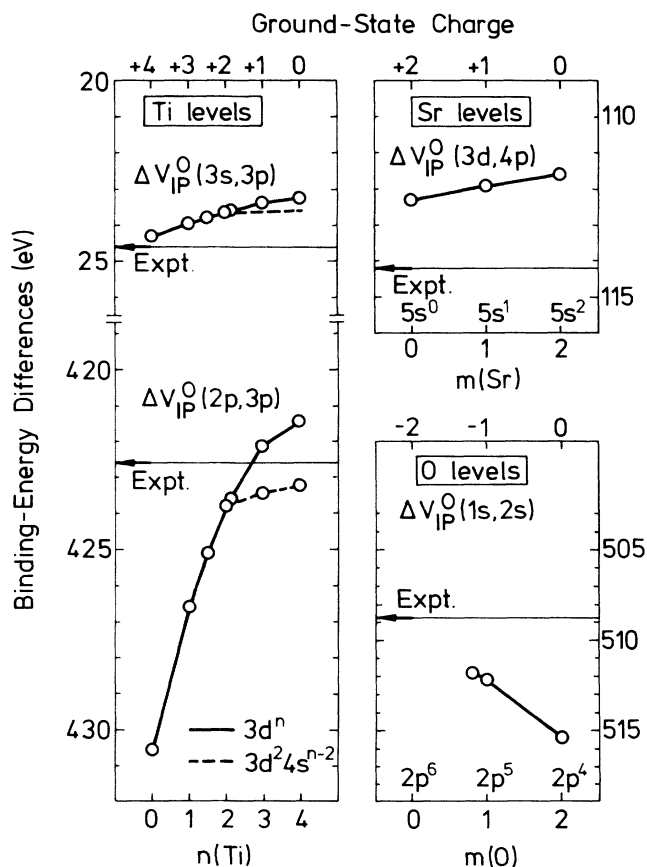


FIG. 8. Ionization potential differences  $\Delta V_{IP}^0$  for the Ti, Sr, and O atoms (chemical ions) as function of the ground-state valence-orbital occupation numbers (Ti  $3d^n$ , Sr  $5s^m$ , and O  $2p^{6-m}$ ). The corresponding experimental values for SrTiO<sub>3</sub> are indicated by arrows.

and experiment is to compare BE differences for different core electrons in a particular type of ion and for cation and anion electrons, respectively. This procedure avoids the reference-level problem. One might also hope that these checks reduce experiment-theory disagreements due to the not well-known correction terms. Figures 8 and 9 show differences  $V_{IP}^0$  for Ti, Sr, and O levels as a function of the valence-orbital occupation numbers. In the first case one is free from Madelung potentials, because in an electrostatic field the different electrons of one type of atom should be shifted by the same amount from their free-atom values. For titanium the (3s)-(3p) separation is nearly constant, whereas the (2p)-(3p) distance shows a steep gradient allowing an approximate determination of the Ti 3d occupation number. Accepting a maximum deviation between experiment and theory of about +2 eV, a Ti  $3d^{1.5}$  state ( $Ti^{2.5+}$ ) or an even higher 3d occupation is determined for the ground state in agreement with the conclusions drawn above. The Sr ground state cannot be found out because of the flatness of the theoretical  $V_{IP}^0(m)$  curve. Due to the lack of  $O^{2-}$  data, no reliable conclusion can be drawn from the O 1s-O 2s distance for the oxygen valence state in  $SrTiO_3$ . However, the theoretical O 1s-O 2p difference for  $O^{1.2-}$  (525.6 eV, see Table IV) agrees rather well with the experimental value of 525.0 eV (the center of gravity of the VB is at 6 eV).<sup>17</sup> A 2p occupation with only about five electrons is therefore a reasonable value.

In Fig. 9 we compare the theoretical and experimental

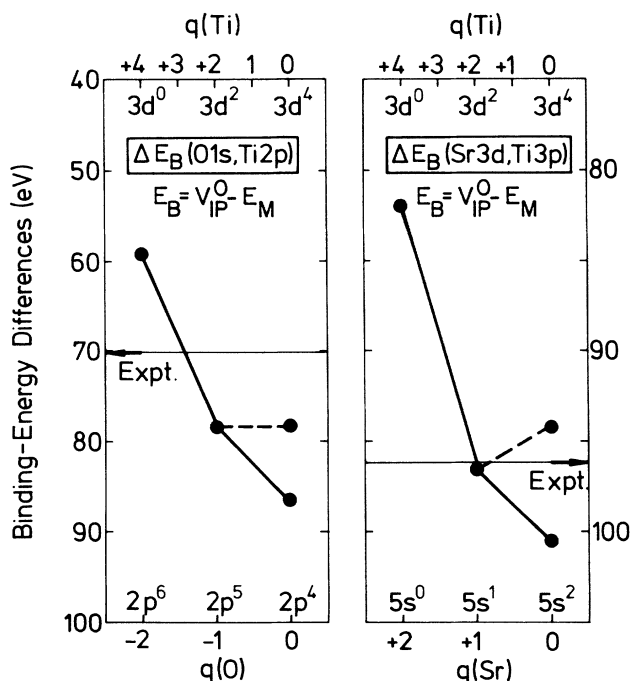


FIG. 9. Calculated binding-energy differences  $\Delta E_B = \Delta V_{IP}^0 - \Delta E_M$  in different atoms (chemical ions) as a function of the ground-state charges. Compare with Fig. 8. The values connected with dashed lines represent the Ti  $3d^{2.5}$  ground state. The corresponding experimental values in  $SrTiO_3$  are indicated by arrows.

binding-energy differences of core electrons on different atoms. As is evident, the pure ionic picture is far away from experiment. It follows again that the Ti 3d occupation is about  $n=1.5$  [ $n=1$  from BE(O 1s, Ti 2p) and  $n=2$  from BE(Sr 3d, Ti 3p)], and that the oxygen and strontium charges are strongly reduced as compared to their formal values.

## V. SURFACE CORE-LEVEL SHIFTS

In the surface plane the electronic structure is modified because of the reduced coordination. Additional charge may concentrate at the Ti sites due to the missing electronegative oxygen neighbor (Fig. 2). This effect may be described in terms of a surface-enhanced covalency (SEC).<sup>14</sup> SEC decreases the effective atomic charges because of an increase (decrease) of the Ti 3d (O 2p) orbital occupation in the surface layer ( $3d^n \rightarrow 3d^{n+\Delta n}$  and  $2p^{6-m} \rightarrow 2p^{6-(m+\Delta m)}$ , respectively). SEC of course produces a surface core-level shift. Within the LHPI model the theoretical surface core-level shift (SCLS) is given by the formula

$$\Delta E_B = \Delta V_{IP}^0 - \Delta E_M, \quad (5.1)$$

$$\Delta V_{IP}^0 = V_{IP}^0(n + \Delta n) - V_{IP}^0(n).$$

$\Delta V_{IP}^0$  accounts for bulk-surface differences in the free-atom contribution to the binding energy and  $\Delta E_M$  represents the Madelung shift from Eq. (3.13). We neglect any surface structure relaxations as have been observed in a recent LEED study<sup>36</sup> and assume ideally terminated surfaces (Fig. 2). We further neglect bulk-surface differences in the compression and screening terms, which presumably cancel in taking BE differences. For nonintegral  $\Delta n$ ,  $\Delta V_{IP}^0$  is taken from a parabolic fit to the  $V_{IP}^0$  values shown in Figs. 4 and 6. Figure 10 shows the SEC effect on the Ti 3p BE for values of  $\Delta n$  varying between 0 and 1 in dependence on the bulk 3d occupation  $n$ . Neglecting SEC ( $\Delta n=0$ ), this model predicts higher surface binding energies due to the pure Madelung shift, and this is in contradiction to experiment (Fig. 1). Inclusion of SEC lowers the theoretical BE's, and for realistic values of  $n$  between 0 ( $Ti^{4+}$ ) and 2 ( $Ti^{2+}$ ) one has to assume a considerable surface enhancement of  $\Delta n=0.5$ . As is seen from Figs. 10 and 5 the values  $n=1.5$  and  $\Delta n=0.6$  are in good agreement with both the bulk BE and the surface shift. We point to that  $\Delta n$  can be determined very accurately within our simple model because  $\Delta n=0.47$  already corresponds to  $n=0$  in order to give the correct shift, and the latter value is far away from experiment as concerns the bulk BE (see Fig. 5).

Elliatioglu and Wolfram<sup>13</sup> have predicted SEC for  $SrTiO_3(001)$  using a linear combination of atomic orbitals (LCAO) model for the description of the bands with  $\pi$  character ( $dt_{2g}$  orbitals). According to their model, an additional electron can reside on each surface Ti cation, even though band-gap surface states, which are not found in PE experiments,<sup>16</sup> are unoccupied. For  $n$ -type  $SrTiO_3$  with the Fermi level at the bottom of the conduction band (as in our experiments) they found an increase of Ti

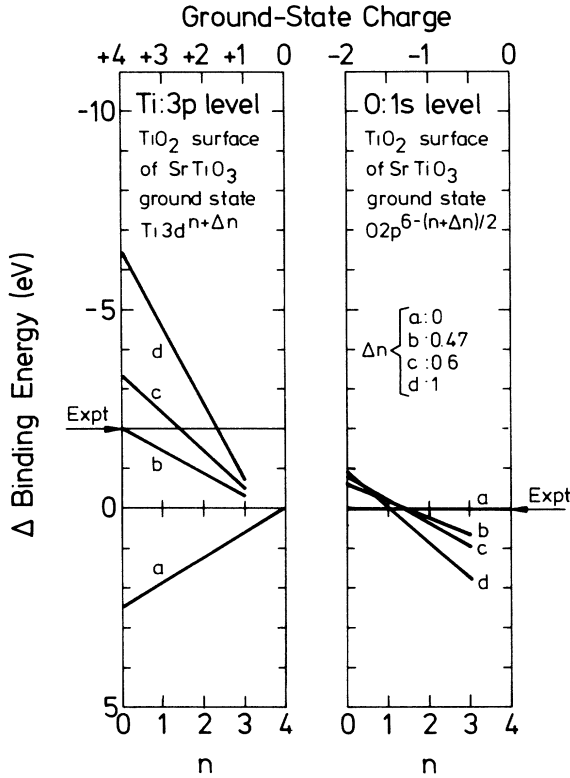


FIG. 10. Calculated surface core-level shifts (SCLS) in the binding energies,  $\Delta E_B = \Delta V_{IP}^0 - \Delta E_M$ , of Ti  $3p$  and O  $1s$  for the TiO<sub>2</sub> plane terminated surface of SrTiO<sub>3</sub>(001) as a function of the ground-state valence-orbital occupation numbers in the bulk [Ti  $3d^n$  and O  $2p^{6-m}$  ( $2m = n$ ), respectively]. As a parameter, the surface-bulk difference in occupation number (effect of the surface enhanced covalency)  $\Delta n$  is varied. The experimental shifts (compare with Fig. 1) are indicated.

$3d$  level occupation from  $n = 1.1$  in the bulk to  $n_s = 1.55$  ( $\Delta n = 0.45$ ) in the surface, which is in excellent agreement with our finding. Cluster calculations<sup>14</sup> have confirmed SEC ( $\Delta n = 0.16$ ), but this effect is not seen in other tight-binding calculations.<sup>15</sup>

The question arises whether the lowering of the Ti  $3p$  BE by 2.0 eV at the surface can be understood in the local  $3d$ -screening model, too. In our opinion, an inspection of the results presented in Fig. 4 shows that this is not possible because of the flatness of the corresponding  $V_{IP}^{scr}$  curve. However, less local  $4sp$  screening behind the main line would be compatible with that experiment.

As concerns the unshifted experimental O  $1s$  BE (Fig. 1) for TiO<sub>2</sub> termination, a small positive shift of some tenth eV is predicted for the maximum SEC effect of  $\Delta n = 0.6$ , which corresponds to a reduction of O  $2p$  occupation in the surface by  $\Delta m = +0.3$  (Fig. 10). In view of the simplicity of our model, this small deviation to experiment seems to be acceptable. It is further seen that O  $2p$  bulk occupations  $m = 0.5 - 0.75$ , corresponding to  $q(O) = -1.5$  and  $q(O) = -1.25$ , respectively, compare best with experiment.

A similar examination is performed for the Sr  $3d$  and

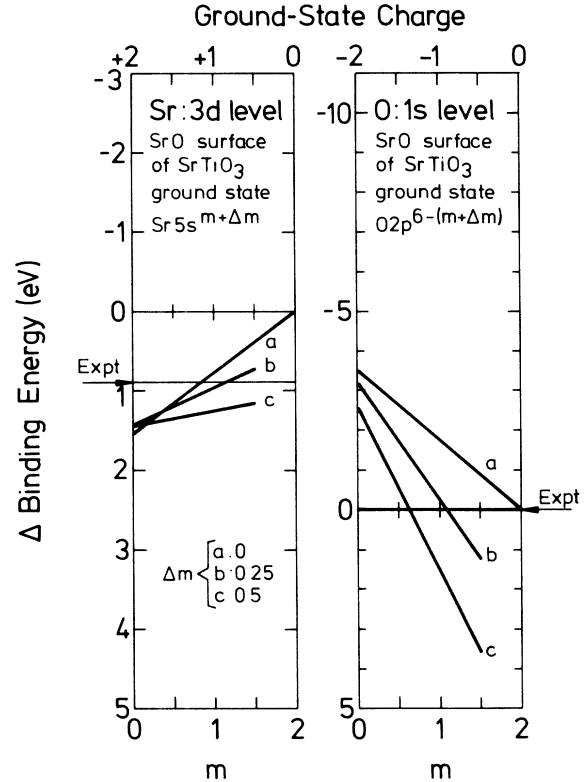


FIG. 11. Same as in Fig. 10 for the Sr  $3d$  and O  $1s$  levels in the SrO-plane terminated SrTiO<sub>3</sub>(001) surface.

O  $1s$  BE's on a SrO-terminated surface (Fig. 11). In order to explain the experimental Sr  $3d$  SCLS of +0.8 eV, no SEC has to be assumed for this surface, if Sr<sup>1.25+</sup> exists in the bulk. This charge is in excellent agreement with the Ti charge 2.5+ deduced above. However, SEC must be concluded from the O  $1s$  energies. An unshifted O  $1s$  line, as seen experimentally, requires an oxygen surface decrease  $\Delta m = 0.5$  for a bulk charge  $q(O) = -\frac{5}{4}$ . This in turn would result in a slightly too high Sr  $3d$  shift. Having in mind the unresolved problem of oxygen BE's, this result should not be taken too seriously. In any case, we deduce from the results of Fig. 11 that a full O  $2p$  valence shell (O<sup>2-</sup>) is not compatible with experiment, which favors the bulk Sr and O charges as deduced from Ti  $3p$  energies,  $q(Sr) = -q(O) = 1.25$ .

## VI. DEFECT-INDUCED CORE-LEVEL SHIFTS

Finally we examine the defect-induced core-level shifts (Fig. 1) in a very rough model. The main defects created by ion-bombardment or heavy anneal in UHV are oxygen vacancies ( $V_O$ ). In creating a bulk  $V_O$  is assumed that the charge of the missing lattice oxygen,  $q(O) = -2(1 - n/4)$ , is equally shared by the two Ti neighbors [Ti(1)], which then increase their  $3d$  level occupation,  $n \rightarrow n + \Delta n_1$  with  $\Delta n_1 = (1 - n/4)$ . These  $3d$  electrons occupy states in the gap, which are seen in experiment as emission  $D_1$ .<sup>17,21,22</sup> This charge redistribution in turn decreases both the ionization potential

$[V_{IP}^0(n) \rightarrow V_{IP}^0(n + \Delta n_1)]$  and the Madelung potential  $[\Delta E_M = -3(e^2/2a)\Delta n_1]$  of the corresponding two reduced Ti atoms. Again both shifts act oppositely and the combined effect is shown in the left panel of Fig. 12 as a function of the ground-state Ti 3d occupation number. The covalency shift dominates the Madelung shift and a lowering of the Ti 3p binding energy is calculated as is observed in experiment (lines  $T_1$  and  $T_2$  in Fig. 1). Agreement with the experimental shift is achieved for  $n = 1.4$ , whereas the pure ionic picture ( $n = 0$ ) is far away from experiment. Although this Ti 3d ground-state occupation is perfectly within the limits for  $n$  estimated above, this value should not be overestimated because of the roughness of the charge redistribution model used, which, however, yields the right tendency. Furthermore, the detailed line structure behind the broad Ti 3p defect emission  $T_1$  is unresolved and the very surface-sensitive study represented in Fig. 1 requires a supplementary bulk investigation with XPS, which is in progress.<sup>39</sup> Disregarding these restrictions, one may say that the reduced Ti atoms represent the  $Ti^{2+}$  ( $n = 1.4$ ) or  $Ti^{1.5+}$  ( $n = 2$ ) species and not the  $Ti^{3+}$  species of the formal-valence picture.

Just above we have assumed a bulk origin (including the second layer) of the  $V_O$ -induced Ti 3p emission  $T_1$ . Ti- $V_O$  complexes may also occur in the surface plane.

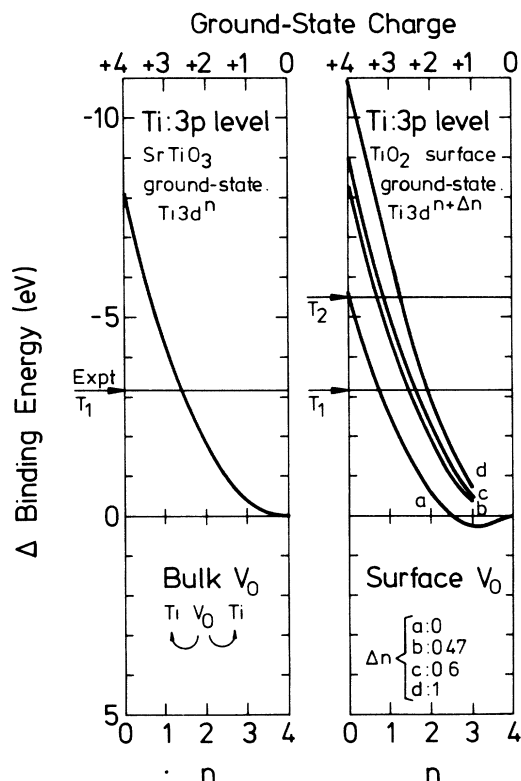


FIG. 12. Calculated oxygen-vacancy induced shift of the Ti 3p core-level binding energy,  $\Delta E_B = \Delta V_{IP}^0 - \Delta E_M$ . Left: Oxygen vacancy in the bulk (including the second layer). Right: Oxygen vacancy in the  $TiO_2$  surface. Compare with Fig. 10.  $T_1$  and  $T_2$  represent the experimentally observed shifts (see Fig. 1).

The corresponding theoretical shift for the  $TiO_2$  surface of  $SrTiO_3$  is given in the right panel of Fig. 12. The calculation is as above, but SEC is taken into account. An enhancement of the Ti 3d occupation from  $n = 1.3$  to  $n = 1.3 + 0.5 = 1.8$  in the surface is compatible with the experiment, but a much stronger SEC by about  $\Delta n = 1$  cannot be excluded from this experiment. However, the latter value is very unlikely as judged from the surface core-level shift. It is not completely clear from experiment whether  $T_1$  represents pure bulk or surface vacancies, respectively, because oxygen adsorption does not completely suppress the defect emissions.<sup>8</sup> From the results of Fig. 12 one might imagine that both bulk and surface oxygen vacancies are behind the Ti 3p emission  $T_1$  and the Ti 3d gap emission  $D_1$ .

An inspection of Fig. 12 shows that emission  $T_2$  ( $\Delta E_B = -5.5$  eV, Fig. 1) may also arise from Ti- $V_O$  complexes. However, this would require a much higher ionicity in contradiction to the results from the binding energies in the stoichiometric compound. Furthermore, this interpretation would let the defect emission  $T_1$  go unexplained. We ascribe  $T_2$  and  $D_2$  (Fig. 1) to metallic Ti clusters on the surface because these emissions only occur after a very heavy anneal<sup>8</sup> and its BE shift just corresponds to the shift in going from  $SrTiO_3$  bulk to Ti metal. Here a comparison with experimental results from defective  $TiO_2$  is instructive. Rocker and Göpel<sup>27</sup> have found five effective oxidation states for Ti on  $TiO_2(110)$  covered with two monolayers of Ti metal and have ascribed them to  $Ti^{4+}$ ,  $Ti^{3+}$ ,  $Ti^{2+}$ ,  $Ti^{1+}$  (this labeling does not give the effective valences) and  $Ti^0$  (metal). Their " $Ti^{4+}-Ti^0$ " shift of 5.1 eV is in good agreement with the  $T_2$  shift in  $SrTiO_3$  and thus supports our assumption of metallic Ti clusters behind the emission  $T_2$ . Furthermore, the filling of the band gap of  $TiO_2$  with Ti 3d states after evaporation of two monolayers of Ti has just the shape of our band-gap emission  $D_2$ .

## VII. SUMMARY

We compare our results for the effective charges in  $SrTiO_3$  with existing theories for the electronic structure of this compound (Table VI). Weyrich and Siems<sup>10</sup> have performed calculations based on the density-functional theory and the LMTO method and have found a Ti 3d contribution of about 1.7 electrons to the bulk valence band. Our finding that the core-level binding energies are best explained with a Ti 3d occupation between 1.5 and 2.0 electrons is in excellent agreement with this result from band theory. Furthermore, Weyrich and Siems<sup>10</sup> also found a high Sr 5p contribution of 0.8 electrons. This again is in astonishing agreement with our study, although we have assumed an occupation of the 5s level in comparing our calculations with experiment. This agreement between band theory and photoemission results for a transition-metal oxide answers some questions posed in the Introduction: core-level photoemission is able to deduce ground-state properties such as effective charges and the results are in agreement with band calculations. Table VI gathers electronic valence charges as derived from different electronic structure calculations.<sup>10,13-15</sup>

TABLE VI. Electronic valence charges of bulk and surface titanium, oxygen, and strontium atoms in SrTiO<sub>3</sub> as derived from theory.

	Bulk	(001)TiO <sub>2</sub> surface	(001) SrO surface
Ti(3d <sup>n</sup> )	1.7 <sup>a</sup>		
	1.58 <sup>b</sup>	1.48 <sup>b</sup>	1.61 <sup>b</sup>
	1.65 <sup>c</sup>	1.81 <sup>c</sup>	(subsurface)
	1.1 <sup>d</sup> (3d <sub>t<sub>2g</sub></sub> )	1.55 <sup>d</sup> (3d <sub>t<sub>2g</sub></sub> )	
O(2p <sup>m</sup> )	5.2 <sup>a</sup>		
	5.47 <sup>b</sup>	5.43 <sup>b</sup>	5.7 <sup>b</sup>
	5.73 <sup>c</sup>	5.66 <sup>c</sup>	
Sr(5s <sup>m</sup> )	0.8 <sup>a</sup>		

<sup>a</sup>Reference 10.<sup>b</sup>Reference 15.<sup>c</sup>Reference 14. (Ti<sub>2</sub>O<sub>10</sub> cluster, results depend on cluster type).<sup>d</sup>Reference 13.

For the bulk charges we consider the values of Weyrich and Siems<sup>10</sup> as the most reliable ones because of the advanced method used by these authors. Surface-enhanced covalency has been predicted by Ellialtioglu and Wolfram<sup>13</sup> and confirmed to a lesser extent in the cluster study of Tsukada, Satoko, and Adachi,<sup>14</sup> but has not been found by Toussaint, Selme, and Pecheur.<sup>15</sup> Our core-level study here and our results from Ti 3d resonant photoemission<sup>17</sup> prove the existence of SEC and even quantitatively confirm the calculation of Ref. 13 ( $\Delta n = 0.5$ ).

On the one hand our results are not so surprising: An inspection of Ti 2p binding energies including the metal (containing effectively Ti<sup>0</sup> species) and ionic compounds as Ni<sub>2</sub>TiF<sub>6</sub>, where the assumption of Ti<sup>4+</sup> species is a

good approximation, as given in Ref. 1 on page 68, reveals a chemical shift of about 2 eV per oxidation state. The SrTiO<sub>3</sub> to Ti-metal shift is about 5 eV and thus leads to an effective Ti charge of +2.5 in SrTiO<sub>3</sub>. This is just the value as deduced from our study. On the other hand, it is astonishing that our rough point-ion model works so well for SrTiO<sub>3</sub>, where covalency is found to be rather high.

#### ACKNOWLEDGMENTS

This work was supported by the Bundesminister für Forschung und Technologie (Bonn, Germany) and the Deutsche Forschungsgemeinschaft (Bonn, Germany).

<sup>1</sup>C. D. Wagner, W. M. Riggs, L. E. Davies, and J. F. Moulder, in *Handbook of X-Ray Photoelectron Spectroscopy*, edited by G. E. Muilenberg (Perkin Elmer Corp., Eden Prairie, Minn., 1979).

<sup>2</sup>C. S. Fadley, S. B. M. Hagström, M. P. Klein, and D. A. Shirley, *J. Chem. Phys.* **48**, 3779 (1968).

<sup>3</sup>P. H. Citrin and T. D. Thomas, *J. Chem. Phys.* **57**, 4446 (1972).

<sup>4</sup>G. D. Mahan, *Phys. Rev. B* **22**, 3102 (1980).

<sup>5</sup>G. D. Mahan, *Phys. Rev. B* **21**, 4791 (1980).

<sup>6</sup>J. Q. Broughton and P. S. Bagus, *Phys. Rev. B* **30**, 4761 (1984); **36**, 2813 (1987).

<sup>7</sup>W. F. Egelhoff, *Surf. Sci. Rep.* **6**, 253 (1987).

<sup>8</sup>B. Cord and R. Courths, *Surf. Sci.* **162**, 34 (1985).

<sup>9</sup>N. B. Brookes, G. Thornton, and F. M. Quinn, *Solid State Commun.* **64**, 383 (1987).

<sup>10</sup>K. A. Weyrich and R. Siems, *Jpn. J. Appl. Phys.* **24**, Suppl. **2**, 206 (1985).

<sup>11</sup>D. K. G. de Boer, C. Haas, and G. A. Sawatzky, *Phys. Rev. B* **29**, 4401 (1984).

<sup>12</sup>B. W. Veal and A. P. Paulikas, *Phys. Rev. B* **31**, 5399 (1985).

<sup>13</sup>S. Ellialtioglu and T. Wolfram, *Phys. Rev. B* **18**, 4509 (1978).

<sup>14</sup>M. Tsukada, C. Satoko, and H. Adachi, *J. Phys. Soc. Jpn.* **48**, 200 (1980); *Prog. Surf. Sci.* **14**, 113 (1983).

<sup>15</sup>G. Toussaint, M. O. Selme, and P. Pecheur, *Phys. Rev. B* **36**,

6135 (1987).

<sup>16</sup>V. E. Henrich, *Rep. Prog. Phys.* **48**, 1481 (1985).

<sup>17</sup>R. Courths, B. Cord, and H. Saalfeld, *Solid State Commun.* **70**, 1047 (1989).

<sup>18</sup>E. Bertel, R. Stockbauer, and T. E. Madey, *Phys. Rev. B* **27**, 1937 (1983); *Surf. Sci.* **141**, 355 (1984).

<sup>19</sup>K. E. Smith and V. E. Henrich, *Solid State Commun.* **68**, 29 (1988).

<sup>20</sup>N. B. Brookes, D. S.-L. Law, T. S. Padmore, D. R. Warburton, and G. Thornton, *Solid State Commun.* **57**, 473 (1986).

<sup>21</sup>V. E. Henrich, G. Dresselhaus, and H. J. Zeiger *Phys. Rev. B* **17**, 4908 (1978).

<sup>22</sup>W. J. Lo and G. A. Somorjai, *Phys. Rev. B* **17**, 4942 (1978).

<sup>23</sup>C. N. Sayers and N. R. Armstrong, *Surf. Sci.* **77**, 301 (1978).

<sup>24</sup>S. Ferrer and G. A. Somorjai, *Surf. Sci.* **94**, 41 (1980).

<sup>25</sup>R. G. Egdell and P. D. Naylor, *Chem. Phys. Lett.* **91**, 200 (1982).

<sup>26</sup>W. Göpel, D. Frankel, M. Jaehnig, K. Phillips, J. A. Schäfer, and G. Rocker, *Surf. Sci.* **139**, 333 (1984).

<sup>27</sup>G. Rocker and W. Göpel, *Surf. Sci.* **181**, 530 (1987).

<sup>28</sup>R. Heise, R. Courths, K. Göhler, and J. Noffke (unpublished).

<sup>29</sup>D. D. Koelling and B. N. Harmon, *J. Phys. C* **10**, 3107 (1977).

<sup>30</sup>H. Gollisch and L. Fritsche, *Phys. Status Solidi B* **86**, 145 (1978).

- <sup>31</sup>L. Fritsche and H. Gollisch, *Z. Phys. B* **48**, 209 (1982).
- <sup>32</sup>L. Fritsche and H. Gollisch, in *Local Density Approximations in Quantum Chemistry and Solid State Physics*, edited by J. P. Dahl and J. Avery (Plenum, New York, 1984).
- <sup>33</sup>M. P. Tosi, in *Solid State Physics*, edited by H. Ehrenreich, D. Turnbull, and F. Seitz (Academic, New York, 1964), Vol. 16, p. 44.
- <sup>34</sup>T. Wolfram, E. A. Kraut, and F. J. Morin, *Phys. Rev. B* **4**, 1677 (1973).
- <sup>35</sup>R. E. Watson, J. W. Davenport, M. L. Perlman, and T. K. Sham, *Phys. Rev. B* **24**, 1791 (1981).
- <sup>36</sup>N. Bickel, G. Schmidt, K. Heinz, and K. Müller, *Phys. Rev. Lett.* **62**, 2009 (1989).
- <sup>37</sup>Veal and Paulikas (Ref. 12) use the term “nonlocal screening” for these processes. To avoid confusion with the polarization-screened “bare” hole in the electrostatic model used here, we do not use this term.
- <sup>38</sup>H. Eckardt and L. Fritsche, *J. Phys. F* **17**, 1795 (1987).
- <sup>39</sup>This known fact has been demonstrated for chromium in Ref. 12.
- <sup>40</sup>H. Van Doveren and J. A. Th. Verhoeven, *J. Electron Spectrosc. Relat. Phenom.* **21**, 265 (1980).